

Development of Thomson Scattering Measurement System for Long Duration Discharges on the QUEST Spherical Tokamak

Kaori KONO, Takeshi IDO, Akira EJIRI¹⁾, Kazuaki HANADA, Qilin YUE, Makoto HASEGAWA, Yi PENG¹⁾, Seiya SAKAI, Ryuya IKEZOE, Hiroshi IDEI, Syoji KAWASAKI, Kengoh KURODA, Takumi ONCHI, Yoshihiko NAGASHIMA and Seowon JANG¹⁾

Kyushu University, Kasuga 816-8580, Japan

¹⁾*The University of Tokyo, Kashiwa 277-8561, Japan*

(Received 13 December 2022 / Accepted 18 January 2023)

The Thomson scattering control system has been modified to measure the time evolution of the electron density and temperature profiles during long duration discharges in the QUEST spherical tokamak. The system consists of a signal generator and a control circuit. The former accepts a QUEST main trigger and provides multiple triggers, each of which starts a short-term (e.g. 15 s) measurement. The latter provides triggers to synchronize the oscilloscope and laser oscillation during a short-term measurement. The system was used in 1000 s long duration discharges in QUEST, and the temporal evolutions of density and temperature profiles were obtained successfully. It was found the profiles are stationary after about 300 s.

© 2023 The Japan Society of Plasma Science and Nuclear Fusion Research

Keywords: long duration discharge, Thomson scattering, spherical tokamak, hot wall, steady state plasma, QUEST

DOI: 10.1585/pfr.18.1405012

1. Introduction

One of the issues in nuclear fusion research is the steady state operation. In steady state plasma, the plasma wall interaction which determines the particle recycling becomes important, because it has a much longer time scale than those in core plasma. Thus, long duration discharge experiments are necessary for the fusion research. Long duration discharges have been performed in several devices, such as Tore Supra [1], TRIAM-1M [2], LHD [3, 4], and EAST [5], all of which have reported that plasmas are sustained for durations sufficiently longer than the characteristic time scales of transport in core plasmas, such as the energy confinement time and the current diffusion. However, TRIAM-1M reports that the discharges are terminated because the density becomes uncontrollable due to the increase in the particle recycling from the plasma-facing components. In QUEST spherical tokamak, the temperature of plasma-facing metal wall (called hot wall) can be heated up to 400°C to control the recycling. An 8.2 GHz (40 kW) microwave source has been used to launch EC wave, which enables long duration discharges [6]. Experiments have been conducted at various wall temperatures using the hot wall [7]. On the other hand, it is known that the plasma does not reach a steady state even during these long runs in some discharges. Thus, it is important to measure the time variation of plasma parameters. In long duration discharges, the measurement of electron density and electron temperature by Thomson scattering (TS) is essential, but has not been realized in

QUEST so far. The main reason was that the main trigger from the QUEST operating system to TS measurement system was only once per shot, and the system could only measure for a short time (a few 10 s), which is limited by the memory size of the fast oscilloscopes [8]. To solve the problem, the control system was improved.

This paper describes the newly developed control system, and the time evolutions of the electron density and electron temperature profiles were obtained by the system for the first time in the long duration discharges (1000 s) in QUEST. Section 2 describes the TS measurement technique for long duration discharges, and the results are shown in Sec. 3. Finally, Sec. 4 summarizes the results.

2. New TS Measurement System

Firstly, the TS system and the previous data acquisition sequence are described briefly, and then a new control system is described. The TS system in QUEST is similar to that in the TST-2 spherical tokamak [9]. The signals from six fast response polychromators [10] are directly recorded by six fast oscilloscopes (Yokogawa Electric Co., DL7480 or DLM4058), which accept multiple triggers. The number of acceptable triggers is limited by the memory size, and it is a few hundreds. In the following explanation, we assume it is 150. An oscilloscope records the signal for 1 μ s for each laser pulse, which is operated at 10 Hz. Then the number of 150 triggers corresponds to the measurement period of 15 s. After the 150 triggers, all the stored data in an oscilloscope is transferred to a remote PC automati-

author's e-mail: kono@triam.kyushu-u.ac.jp

cally. This one sequence of data acquisition corresponds to one subshot operation in the new system described in the following. We constructed a new system, in which many subshot operations are repeated during a long duration discharge.

Figure 1 shows the newly developed control and data acquisition system for long duration discharges. There are two improvements from the previous system. One is the signal generator (SG) shown in blue, and the other is Raspberry Pi shown in magenta in Fig. 1. SG receives the main trigger and generates a subshot trigger and a gate signal for the oscilloscope at a specified time interval ΔT_s (typically $\Delta T_s = 60$ s). The subshot is a concept to distinguish multiple measurement periods during a single discharge. Upon receiving this subshot trigger, the control circuit (CC) generates trigger signals (at 10 Hz) that synchronize the oscilloscope data acquisition and the laser's flash lamp timing. Note that the laser's flash lamp timing (at 10 Hz) provided by CC is reset at each subshot trigger, and the first flash lamp trigger occurs 0.1 s after the subshot trigger. The oscilloscope starts data acquisition when the first flash lamp is triggered. After a given number of triggers, which is 150 in the above explanation, all the oscilloscopes' stored data in this subshot are transferred to a remote PC via LAN. This subshot operation is repeated during a long duration discharge. The measurement time is delayed by the delays in SG ($0.7 \pm 0.01 \mu\text{s}$), CC ($2.5 \pm 0.035 \mu\text{s}$), laser ($270.25 \pm 0.06 \mu\text{s}$). Considering these delays, the actual measurement time t is written as

$t = N_s \times \Delta T_s + (0.7 \pm 0.01) \mu\text{s} + (2.5 \pm 0.035) \mu\text{s} + (270.25 \pm 0.06) \mu\text{s} + N \times 100 \text{ ms}$ ($N_s = 0, 1, 2, \dots, N = 1, 2, \dots$). N_s and N represent the subshot pulses and pulse number, respectively. A Raspberry Pi was introduced to automatically control the laser operation as follows. The Raspberry Pi checks QUEST Sequence Information on web to get the elapsed time (negative for count down and positive for count up) from the start of a discharge. It activates the laser oscillation 15 s before the start of a subshot to stabilize the output, and stops the oscillation 5 s after the subshot. Since the data transfer time for six oscilloscopes

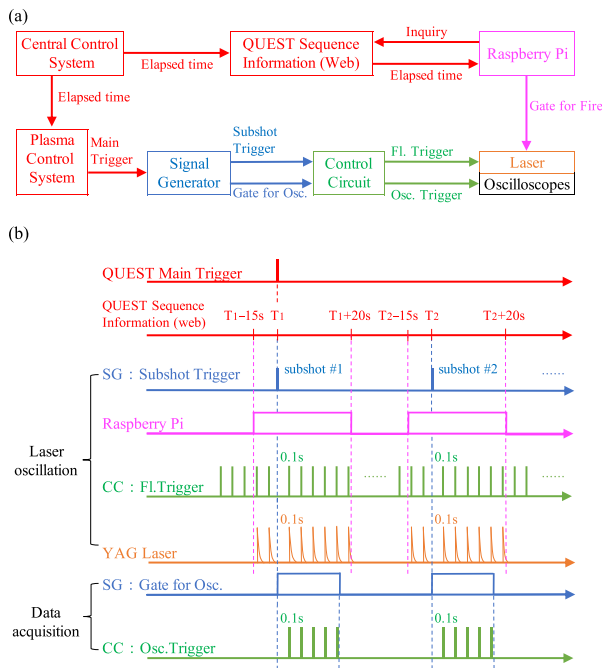


Fig. 1 Conceptual diagram (a) and timing chart (b) of the trigger system for control and data acquisition for TS measurements. In (b), SG stands for Signal Generator and CC for Control Circuit.

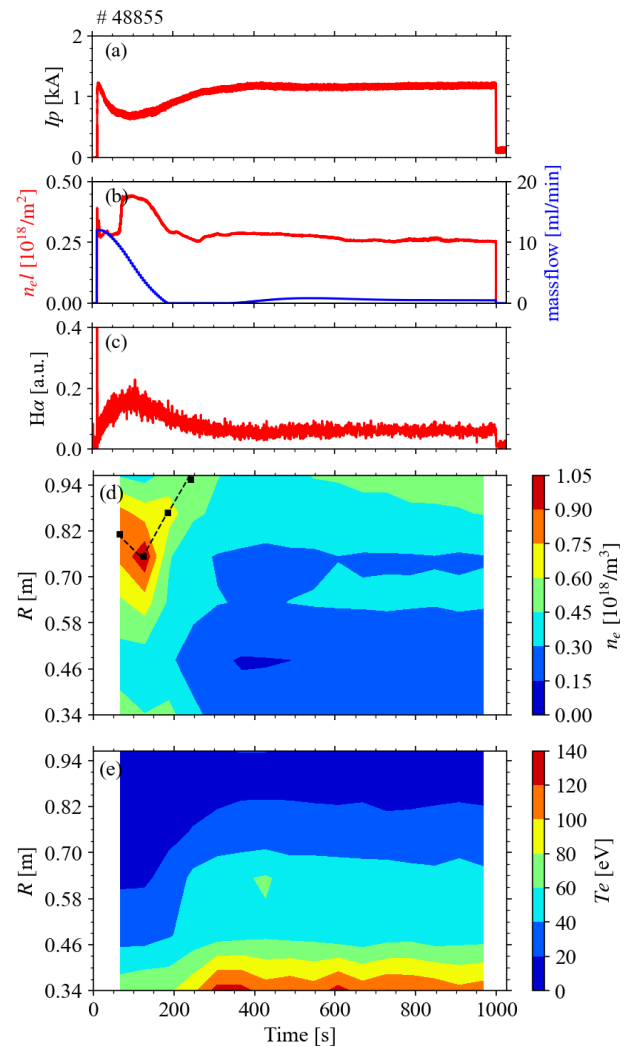


Fig. 2 Discharge waveforms. Plasma current I_p (a), line-integrated density $n_e L$ and particle supply (mass flow rate) (b), H_α emission intensity (c), electron density n_e (d) and electron temperature T_e (e) obtained by TS measurements are shown. The 6 TS measurement positions range from $R = 0.340$ m to $R = 0.965$ m. The subshot interval ΔT_s is 60 s, and each subshot data (15 s) are accumulated to improve the SN ratio. The dots in (d) indicate the location of the maximum density among the 6 positions until 240 s. The plasma is produced by ECH from 11.8 s to 999.0 s. I_p (a) was calculated from Hall effect sensors and equilibrium calculations.

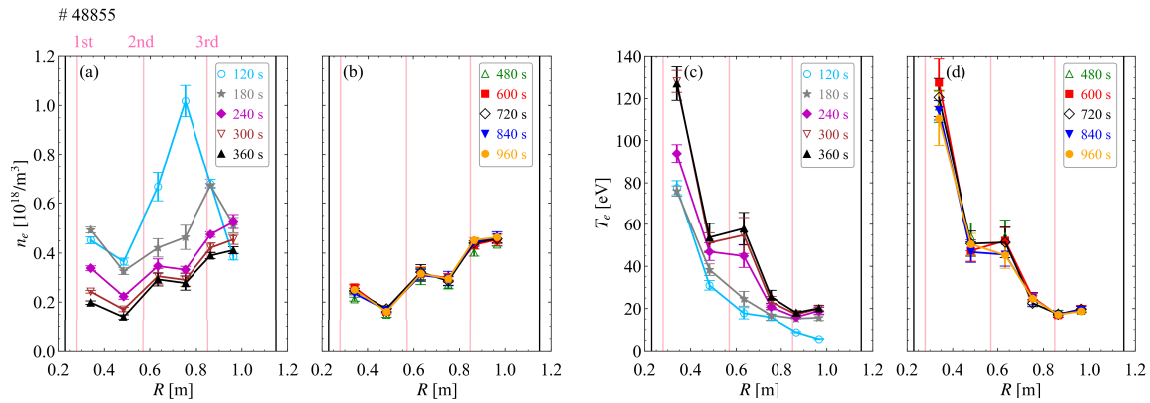


Fig. 3 Spatial profiles of electron density n_e (a), (b) and temperature T_e (c), (d) during the long duration discharge shown in Fig. 2. The subshot interval is 60 s, and only representative profiles are plotted. The black vertical lines on the left and right indicate the inboard and the outboard limiter positions, and the pink vertical lines indicate the resonance layer positions: $R_{1st} = 0.28$ m, $R_{2nd} = 0.57$ m, $R_{3rd} = 0.85$ m.

is about 40 s and the typical subshot measurement time is 15 s, the minimum subshot interval ΔT_s is about 60 s. If we use many (e.g. six) PCs then we can shorten ΔT_s . The upper limit of the pulse number of SG is about 1 million, which means the upper limit of subshot trigger is about 17000 hours. Since the data volume transferred from the oscilloscope per subshot is approximately 26 MB, this may impose the practical limitation. For example, 24-hour discharge requires 1440 ($= 60 \times 24$) subshots, and the required data capacity would be about 37 GB. The new Thomson scattering system is sufficient for the longest duration discharges so far on QUEST (~ 6 hours).

This system was applied to a long duration (1000 s) discharges of QUEST and the measurement results at $\Delta T_s = 60$ s are described. The first subshot ($N_s = 0$), which is before plasma initiation, is used to calculate the time averaged stray light, and then it is subtracted from the data in the following subshots.

3. TS Measurement Results

Figure 2 shows the discharge waveforms of the plasma sustained by electron cyclotron wave (EC wave) with the frequency of 8.2 GHz. The EC wave is injected from a non-focused antenna that causes a considerable poloidal and toroidal spread. The injected EC wave power for this discharge was 20 kW, and the temperature of the hot wall was 200°C. The plasma current I_p became constant after $t = 400$ s and was 1.2 kA. The line-integrated density $n_e l$ remained almost constant at $0.29 \times 10^{18}/\text{m}^2$ after 300 s. Particle supply is feedback controlled from 25.0 s based on H_α emission intensity. The H_α emission intensity has a good correlation with the ionization rate of hydrogen atoms, which means that the incident flux of hydrogen ions is kept constant in this control [11, 12]. Particle supply decreased with time to almost zero after 200 s, and kept no significant level to the end of the discharge (Fig. 2 (b)). This indicates

that the hydrogen atoms or molecules recycled from the plasma-facing wall increase with time [6]. The H_α emission intensity peaks at around 100 s, and decreases with the rise of the plasma current, and is controlled at a constant level from 300 s onward. Figures 2 (d) and 2 (e) show the time variation of electron density n_e and electron temperature T_e measured by the TS system, respectively. The electron density around $R = 0.753$ m increased around 120 s, and the peak moved outward with a gradual decrease. This movement seems to be correlated with the increase in I_p . It was found the profile becomes almost stationary after about 300 s, though the electron density slightly increased at $R \geq 0.9$ m. The electron temperature was increased after 200 s, especially near $R = 0.340$ m, and the profile was almost stationary until 1000 s.

Figure 3 shows the density and the temperature profiles during the long duration discharge shown in Fig. 2. The oscilloscope data was acquired at 10 Hz, but to improve the SN ratio at such a low-density plasma, we accumulated the signals (of 150 pulses) during each subshot data of 15 s. The comparison of $n_e l$ in Fig. 2 (b) and n_e in Fig. 3 indicates that $n_e l$ increase around 100 s is caused by n_e increase at $R = 0.633 - 0.865$ m. The electron density profiles are stationary after 300 s. Figure 4 shows plasma images of long duration discharge at four times: 120 s, 180 s, 300 s, 960 s. At 120 s, when a peculiar electron density profile is observed (Fig. 3 (a)), the plasma was bright and small. At 300 s, when plasma became stationary (Figs. 3 (a) and (c)), the plasma became darker and larger. The plasma was stationary from 300 s to 960 s as seen in the camera image. The boundary position of the bright area estimated from the luminance distribution analysis is consistent with the maximum density position shown in Fig. 2 (d). The electron temperature is high near the fundamental and the second harmonic EC resonance positions ($R_{1st} = 0.28$ m, $R_{2nd} = 0.57$ m) (Fig. 3). The electron temperature at $R = 0.340$ m (near R_{1st}) increases with time

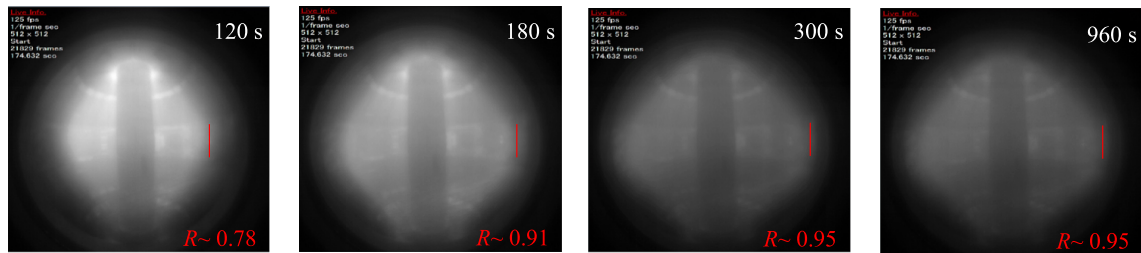


Fig. 4 Plasma images of long duration discharge captured by a high-speed camera. The red line in each image indicates the boundary of the bright area estimated from the luminance distribution analysis, and R is its major radius. The shot number for these images is # 48855.

up to 300 s and remains constant thereafter (see Fig. 2 (e)). The electron temperature at $R = 0.633$ m (near R_{2nd}) also shows a similar time evolution. The electron density and the electron temperature profiles during $t = 300 - 960$ s are almost constant. As a result, the plasma is stationary in terms of I_p , $n_e l$, n_e , T_e -profiles, plasma images during $t = 400 - 960$ s.

4. Conclusions

In order to measure long duration discharges that are a feature of QUEST, a new control system for the Thomson scattering measurement system was developed, allowing measurements at 10 Hz for 15 s every 60 s. When the plasma current become a nearly constant (from about 300 s), the spatial distributions of electron density and electron temperature are found to become stationary.

Acknowledgments

This study was partly supported by National Institute for Fusion Science (NIFS) Collaboration Research Pro-

gram NIFS19KUTR136 and NIFS20KUTR155. We thank Dr. I. Yamada and Dr. Funaba of NIFS for fruitful discussion.

- [1] D. Houtte *et al.*, Nucl. Fusion **44**, L11 (2004).
- [2] H. Zushi *et al.*, Nucl. Fusion **45**, S142 (2005).
- [3] H. Kasahara *et al.*, 25th Int. Conf. Fusion Energy 2014 IAEA-CN-221 (Proc. 25th Int. Conf. Fusion Energy 2014, St. Petersburg, Russian Federation, 2014), IAEA Vienna (2014).
- [4] Y. Yoshimura *et al.*, Nucl. Fusion **56**, 046005 (2016).
- [5] Y. Song *et al.*, IEEE Trans. Plasma Sci. **50**, 4330 (2022).
- [6] K. Hanada *et al.*, Plasma Sci. Technol. **18**, 1069 (2016).
- [7] K. Hanada *et al.*, Nucl. Fusion **57**, 126061 (2017).
- [8] T. Yamaguchi *et al.*, Plasma Fusion Res. **8**, 1302001 (2013).
- [9] T. Yamaguchi *et al.*, Plasma Fusion Res. **5**, S2092 (2010).
- [10] A. Ejiri *et al.*, Plasma Fusion Res. **5**, S2082 (2010).
- [11] M. Hasegawa *et al.*, Fusion Eng. Des. **12**, 202 (2018).
- [12] M. Hasegawa *et al.*, Plasma Fusion Res. **16**, 2402034 (2021).